RESEARCH ARTICLE | OCTOBER 26 2015

Design of electric-field assisted surface plasmon resonance system for the detection of heavy metal ions in water

Htet Htet Kyaw; Sakoolkan Boonruang ; Waleed S. Mohammed; Joydeep Dutta

AIP Advances 5, 107226 (2015)
https://doi.org/10.1063/1.4934934

Design of electric-field assisted surface plasmon resonance system for the detection of heavy metal ions in water

Htet Htet Kyaw,[1] Sakoolkan Boonruang,[2,a] Waleed S. Mohammed,[3,a] and Joydeep Dutta[4]

[1]*Department of Physics, College of Science, Sultan Qaboos University, P. O. Box 36, Al-Khoud 123, Oman*

[2]*Photonics Technology Laboratory, National Electronics and Computer Technology Center (NECTEC), 112 Thailand Science Park, PathumThani 12120, Thailand*

[3]*Center of Research in Optoelectronics, Communication and Control Systems (BUCROCCS), School of Engineering, Bangkok University, PathumThani 12120, Thailand*

[4]*Functional Materials Division, School of Information and Communication Technology, KTH Royal Institute of Technology, Isafjordsgatan 22, SE-164 40 Kista, Stockholm, Sweden*

(Received 23 July 2015; accepted 14 October 2015; published online 26 October 2015)

Surface Plasmon Resonance (SPR) sensors are widely used in diverse applications. For detecting heavy metal ions in water, surface functionalization of the metal surface is typically used to adsorb target molecules, where the ionic concentration is detected via a resonance shift (resonance angle, resonance wavelength or intensity). This paper studies the potential of a possible alternative approach that could eliminate the need of using surface functionalization by the application of an external electric field in the flow channel. The exerted electrical force on the ions pushes them against the surface for enhanced adsorption; hence it is referred to as "Electric-Field assisted SPR system". High system sensitivity is achieved by monitoring the time dynamics of the signal shift. The ion deposition dynamics are discussed using a derived theoretical model based on ion mobility in water. On the application of an appropriate force, the target ions stack onto the sensor surface depending on the ionic concentration of target solution, ion mass, and flow rate. In the experimental part, a broad detection range of target cadmium ions (Cd^{2+}) in water from several parts per million (*ppm*) down to a few parts per billion (*ppb*) can be detected. [http://dx.doi.org/10.1063/1.4934934]

I. INTRODUCTION

Harmful effects of heavy metal ions on environment and human health have always been focus of interest of many researchers.[1] Recently, several studies concerning the detection and removal of heavy metal ions from water have appeared in the literature.[2–6] In order to achieve detection scheme that is practical, it requires a fast and simple sensing system for screening contamination of water bodies especially in remote locations. Several techniques have been applied such as Inductively Coupled Plasma Mass Spectroscopy (ICP-MS),[7] Ion-Selective Electrodes (ISE),[8] Anodic Stripping Voltammetry (ASV),[9] Electrochemical Impedance Spectroscopy (EIS)[10] and Quartz Crystal Microbalance (QCM) Spectroscopy[11] for the detection of heavy metal ions in water samples. Some of the instruments, such as ICP-MS, are very sensitive, but require extensive skills and advanced laboratory facilities. Surface Plasmon Resonance (SPR) offers relatively high sensitivity and it can be applied as a label-free system as well making way for minimal sensing protocols. Sensing techniques based on SPR has thus been implemented in a variety of applications,[12,13] including the detection of heavy metal ion in water.[14–18] SPR techniques have been implemented in portable systems[19–21] that are suitable for on-site analysis. For SPR sensor, the sensing scheme includes the

[a]Corresponding authors: sakoolkan.boonruang@nectec.or.th, waleed.m@bu.ac.th

detection by molecular absorption on a sensor surface, generally via a shift of resonance angle or wavelength. The resonance is caused by electron oscillations on the metal surface which introduces a surface wave called "Surface Plasmon (SP)." At resonance, an incident light is totally absorbed. The resonance condition (incident angle or wavelength) shifts independently on any changes in the refractive index on the metal surface as well as by a deposition of an extra film on the surface. It is worth noting here that as resonance relies on the SP wave, an effective detection distance is within the penetration depth of the SP wave, which is typically around 200 nm from the surface in water. For metal ion detection, several sensing approaches have been designed such as using peptide groups for selective detection of Ni^{2+} and Cu^{2+}ions,[15] using chitosan film for selective detection of Cu^{2+}ions[16] or using enzyme urease as molecular probe for specific detection of Cd^{2+}ions.[17] To minimize the surface functionalization, Wang *et. al.*[18] combined SPR with anodic stripping voltammetry (ASV) where the metal ions were deposited on SPR sensor surfaces by ASV technique. By reading the optical signal shift, detection of Pb^{2+}, Cu^{2+} and Hg^{2+} ions in the range of sub *ppb* to *ppm* levels could be achieved.

In this work, we propose an alternative detection approach by applying an external electrical field to induce ion adsorption on the sensor surface. The technique is referred here as "Electric-Field assisted Surface Plasmon Resonance (EF-SPR)". The optical system utilizes a compact system incorporated within an integrated SPR chip.[21] The Diffractive Optical Elements (DOEs) as fan in/out coupling devices are integrated under the SPR chip. Hence, the detection scheme is set up by capturing an image of a reflected beam without any mechanical movements. At resonance, the reflected beam contains a dark strip indicating an SPR angle. In the current system, the SPR angle is indicated in a certain location on a detector array. For a bulk solution refractive index test, the system showed detection limits down to 10^{-5} Refractive Index Unit (RIU). For the implementation of EF-SPR, one electrode is added on the top of a flow channel while SPR surface (gold film) was used as a working electrode. The system is discussed in detail in sections II and III. Upon the application of an electrical potential to the system, the produced electromagnetic forces drive the ions in the solution onto the gold surface for detection. In section II A, an analytical model is developed where force induced ion mobility in liquid was used to study the time dynamics of the system. The deposition of ion inserts an additional film inducing a refractive index change that varies with time and is proportional to the ionic concentration as well as the type of ions deposited. Thus, the resonance shift is gradually observed over time during the ion deposition. To explain this dynamic response, Maxwell Garnett approximation[22] is used in section II B to theoretically estimate the effective refractive index of the deposited film of ions. In section IV, experimental detection of cadmium ions (Cd^{2+}) in water is demonstrated. The effect of system parameters (flow rate, dimensions of flow channel, and applied potential) on time response is studied. The results show that it is feasible to detect cadmium ions in water with concentration from hundreds of *ppm* down to 250 *ppb*. It is worth mentioning that the detection range (*ppm* to *ppb*) is adapted through the application of appropriate electrical field (controlled by the applied potential and system parameters). Lower force allows for high concentration detection. The detection limit is lowered by maximizing the force via the optimization of the system parameters.

II. ELECTRIC-FIELD ASSISTED SURFACE PLASMON RESONANCE (EF-SPR)

Surface Plasmon (SP) is an electron oscillation at a metal surface. When an incident light has a frequency (and angle) matching the electron oscillation, the light is totally absorbed into electronic surface oscillation that propagates along the metal surface called "Surface Plasmon wave." The phase matching condition between the incident light, or excitation wave, k_{ex} , and the Surface Plasmon wave, k_{sp} , can be written in Eqn. (1) and it is referred as"*Surface Plasmon Resonance (SPR.).*"[12]

$$\sqrt{\frac{\varepsilon_m(\lambda)\,\varepsilon_d(\lambda)}{\varepsilon_m(\lambda)+\varepsilon_d(\lambda)}} \approx \sqrt{\varepsilon_{ex}(\lambda)}\sin\theta_{ex}. \tag{1}$$

where ε_d, ε_m, and ε_{ex} are permittivity of regions as demonstrated in Fig. 1. This phase matching condition exists when the excitation light is *p*-polarized. It is worth noting here that resonance

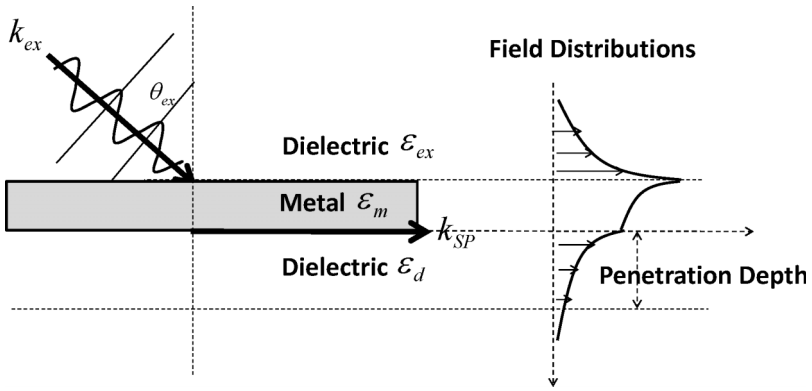

FIG. 1. Schematic representation of phase matching condition of SPR and electric field distribution.

(angle and wavelength) is proportional to permittivity of each media. Based on this scheme, SPR is applied for sensing applications via a detection of permittivity or refractive index change of the film coated on the metal surface within the penetration depth as described in Fig. 1.

For the proposed EF-SPR, the target metal ions are directed onto the sensor surface by the application of an external force (E). As described in Fig. 2, an external electrode is added on top of the flow channel, where sensor's surface behaves as a working electrode. To understand the dynamics of the ion deposition, two models are included in the analysis. Section II A describes an ion mobility model in water, wherein the system parameters are described in Fig. 2. In section II B, time dynamics of SPR shift is included and described using Maxwell Garnett approximation[22] to calculate the change in refractive index during ion accumulation on the electrode.

A. Ion mobility model in water

As demonstrated in Fig. 2, upon inserting a constant electric field to the flow channel, total force applied on each ion in the solution along the y-direction can be written as a difference of electromagnetic force and a resisting force arising from the viscosity of the liquid as in Eqn. (2).

$$F_{tot} = (nqE)\hat{y} - 6\pi r\eta\left(v_x\hat{x} + v_y\hat{y} + v_z\hat{z}\right). \tag{2}$$

Where n is the number of charges, q is the electron charge, and E is the applied electric field ($E = V/d$), V is the applied potential and d is the flow channel thickness. In Eqn. (2), r is the radius of the ion, η is the viscosity of the liquid and v_x, v_y, and v_z are velocity of the ion in x-, y- , and z-directions, respectively. As the solution is fed with a constant flow rate (J) along x- direction, v_x is fixed at J/wd, where w is the width of the channel. Neglecting the z component, v_y changes with time according to the applied voltage that can be expressed as in Eqn. (3).

$$v_y = v_0\left(1 - \exp\left(kt\right)\right). \tag{3}$$

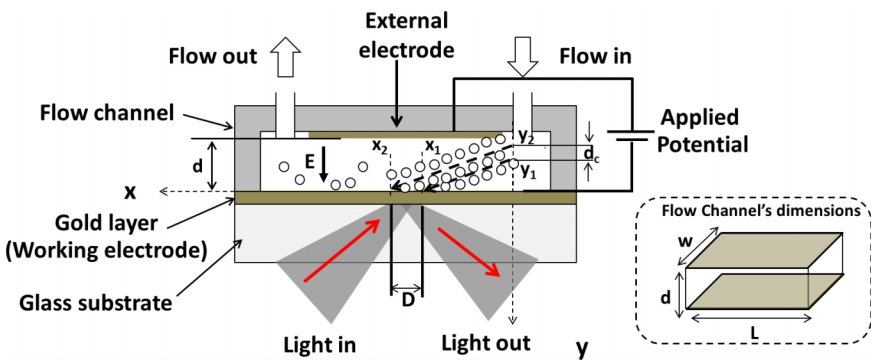

FIG. 2. Schematic representation of the ion mobility in a flow channel including direction of flow and applied potential.

In Eqn. (3), $k = 6\pi r\eta/m$ and $v_0 = nqE/6\pi r$. The velocity reaches steady value v_0 within a very short time and it can hence be assumed to be constant, i.e. $v_y = v_0$. The change of ion position in y direction is then linearly proportional to x as in Eqn. (4).

$$y = \frac{v_x}{v_y}x + y_0. \tag{4}$$

In Eqn. (4), time (t) is related to x through the constant speed v_x, $t = x/v_x$, and y_0 is the original position at $t = 0$ ($x = 0$). As described in Fig. 2, if the incident light forms a spot of width D (located between positions x_1 and x_2) at the gold surface then only the ions flowing between locations y_1 and y_2 in the flow channel can reach this region within a time duration t. The changes in the reflected light are caused by the SPR absorption from the region between x_1 and x_2, or the sensing region in short. SPR signal is only affected by ions adsorbed on the sensing region of width D corresponding to an active region, d_c ($d_c = y_1 - y_2$), in the incident plane ($x = 0$) within which ions contribute to the shift of the SPR signal.

$$d_c = \frac{|v_0|}{v_x}D. \tag{5}$$

Hence, from the flow channel, the ions that are effectively detected has a concentration of

$$C_c = C_0\frac{d_c}{d}. \tag{6}$$

where C_0 is the total ionic concentration (number of ions/m^3).

B. Time dynamics of SPR shift

Based on the ion mobility model, the deposited ions contribute to the shift of the SPR signal and it is directly proportional to the ionic concentration as defined in Eqn. (6) or from the change in an effective refractive index due to the deposited ion layer. To determine the SPR shift, Maxwell-Garnett equation[22] is used for the estimation of the effective dielectric constant (ε_{eff}) of the composite material (metal ions adsorbed on the sensing surface). Here, the metal ions are assumed to be spherical. The size of the metal ions is considered to be within the quasi-static limit ($r_i = 0.01\lambda$). The effective dielectric constant is calculated with respect to the volume fractions (V_f) of the ions that can be expressed as in Eqn. (7). The effective refractive index n_{eff} value then can be defined as $\sqrt{\varepsilon_{eff}}$.

$$\frac{\varepsilon_{eff} - \varepsilon_1}{\varepsilon_{eff} + \varepsilon_1} = V_f\frac{\varepsilon_2 - \varepsilon_1}{\varepsilon_2 + \varepsilon_1}. \tag{7}$$

where ε_1 and ε_2 are the dielectric constants of the host medium (water) and the metal ions respectively. The dielectric function comprises of two optical constants as refractive index (n) and the optical absorption coefficient (k).

To simplify the time dynamic analysis, the rate of change in SPR signal ($dShift/dt$) can thus be expanded as a product of three terms as in Eqn. (8).

$$\frac{dShift}{dt} = \frac{dV_f}{dt} \times \frac{dn_{eff}}{dV_f} \times \frac{dShift}{dn_{eff}}. \tag{8}$$

Where V_f is the volume fraction of the deposited ions, n_{eff} is the effective refractive index of the deposited layer and *Shift* is the SPR signal shift (either unit-less reflection drift in intensity based measurement or resonance-dip spectrum shift in *nm*). It is worth mentioning here that the change of the volume fraction is assumed to be within a constant region of a thickness equivalent to the penetration depth of SP wave in water (~200 *nm*).

In Eqn. (8), the first term indicates the rate of change of the volume fraction of ions in its simplest linear form that can be defined as in Eqn. (9). This representation is however a first order assumption and it is valid only at the linear time dynamics region.

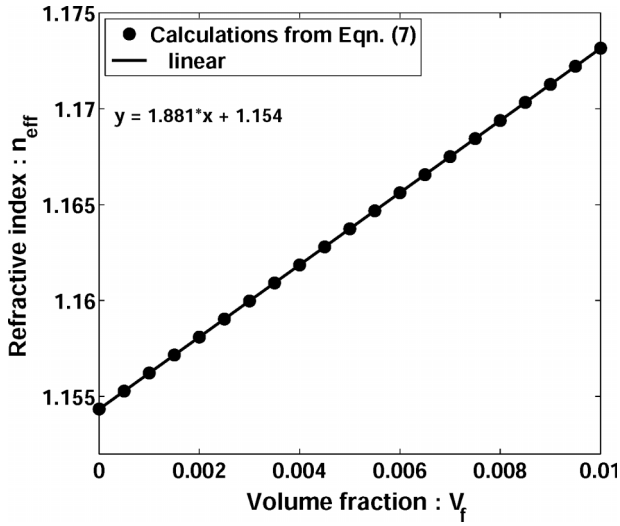

FIG. 3. Change of effective index with ion metal volume fraction for Cd^{2+} ions.

$$\frac{dV_f}{dt} = J \times C_c. \tag{9}$$

As seen, the rate of change of volume fraction of ions is directly proportional to flow rate (J) and concentration of deposited ion (C_c).

The second term in Eqn. (8) introduces the change of the volume fraction with effective refractive index which can be calculated using Maxwell-Garnett equation[22] as in Eqn. (7). For the model, metal ions used in the experiment, cadmium ions, the refractive index (n) and extinction coefficient (k) are n=2.185 and k=5.473, respectively at 660 nm (1.85 eV).[23] The dielectric constant of the host (water), n=1.332512. Figure 3 shows that the calculated n_{eff} increases in almost a linear form with V_f. Thus, the change of volume fraction with effective refractive index can then be considered to be a constant value of 1.881 that is calculated using a linear fitting of the plot in Fig. 3.

The final term in Eqn.(8), which is the change of the signal shift with the bulk refractive index, is measured experimentally by varying the concentration of known solution such as mixture of isopropyl alcohol (refractive index 1.36) and water (refractive index 1.33), for instance. This gives a solution with varying refractive index from 1.33 to 1.36 that will vary from system to system.

In summary, the rate of change in SPR signal is proportional to ionic concentration (C_0) as well as the system parameters such as flow channel dimensions (w, d), flow rate (J), type of metal ion, and limit of detection in SPR system.

III. EXPERIMENT

A. Electrical-Field assisted SPR (EF-SPR) setup

The implemented EF-SPR system is demonstrated in Fig. 4. The optical setup comprises of Light Emitting Diode (LED) as a light source emitting 660 nm wavelength light that is coupled to the system via a multimode fiber. The beam is collimated by a lens before propagating to a 45 degree mirror and an input DOE integrated on the back side of sensor. The input DOE couples incident light to a gold film with the angle corresponding to SPR angle. The reflected beam is then coupled out from the sensor via an output DOE having a mirror pattern to the input DOE. Finally, the reflected beam image is projected on a CMOS camera by a 45 degree mirror followed by an imaging lens as shown. To be able to notice the SPR angle along the reflected beam image, the DOEs behave as lens with high number aperture to ensure that the angular spectrum of the excitation beam covering the SPR spectrum. In addition, a linear polarizer is added to the system to ensure that the excitation beam is p-polarized. The sample's flow channel is located on top of the sensor

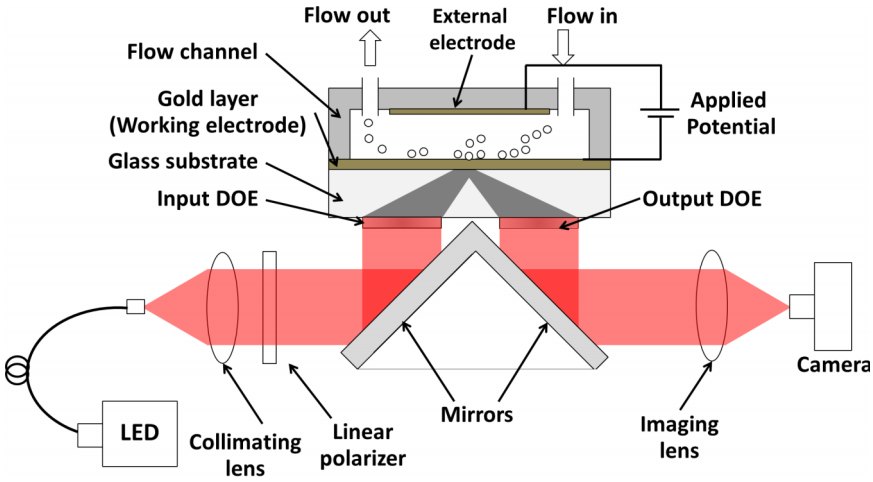

FIG. 4. Schematic representation of the EF-SPR system for metal ion detection.

surface. The dimensions of the flow channel as demonstrated in Fig. 2 are L=1.5 cm, w=0.5 cm, and d = 250 μm. These dimensions are used in the following measurements. The electric force is applied to the sample via one electrode inserted on top of the channel by the extension of another electrode from the sensor surface connected to a DC power supply. The sample is fed at a controlled flow rate by an injection valve pump.

Reflected beam images at "off" and "on" resonance are demonstrated in Fig.5(a) and Fig.5(b), respectively. As demonstrated, dark strip forms along the reflected beam at resonance. This is referred to as "SPR dip" in the figure. The location of the SPR dip shifts with the changes on the sensor surface as demonstrated in a line plot of reflectivity in Fig.5(c). The plot in Fig. 5(c) contains the SPR spectrum when testing with samples having different refractive indices. As observed, resonance can be detected via SPR dip location or reflectivity at certain location along the angular spectrum.

The inset in the figure is a time diagram showing the change of reflectivity at pixel p^{th} =353 in the reflection spectrum when applying solutions (mixture for different concentrations of ethanol and deionized water) with known refractive indices at flow rate 100 $\mu l/min$. There is no applied potential in this measurement. The refractive index (n) of the solutions ($S1$, $S2$, $S3$, $S4$, $S5$ and $S6$) as mentioned in the inset is first measured using a refractometer (ATAGO RX-5000-CX.) Then,

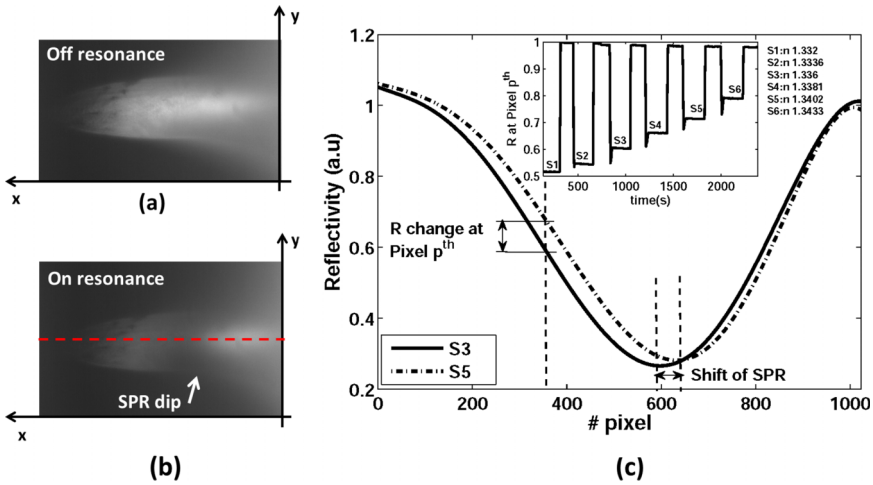

FIG. 5. Reflected beam image at off resonance (a) and on resonance (b) and line plot of resonance spectrum across the reflected beam (c).

the measured sensitivity and the limit of detection are 24.6 a.u/Refractive Index Unit (RIU) and $3.22x10^{-5}$ RIU, respectively. Though this limit is within the commercially available SPR systems, the main scope of this paper is to demonstrate the feasibility of detecting low ion concentrations in the range of ppb utilizing time dynamics and electric field application.

B. Integrated Diffractive Optical Elements (DOEs)-SPR sensors

The integrated DOEs-SPR sensor as shown in Fig. 6(a) comprises of a 2 *mm*- thick BK-7 glass slide (purchased from Foctek Photonics, Inc., refractive index is 1.514 at 660 *nm* wavelength). The slide was coated with 5 *nm*-thick chromium adhesive layer following by 48 *nm*-thick gold layer using magnetron sputtering (AJA International, Inc.; ATC 2000-F). On the back side of the glass slide, DOE patterns fabricated in UV curable hybrid polymer film (OrmoComp from Microresist Technology GmbH) were put. For water having refractive index 1.33, DOEs were designed to couple light at 660 *nm* wavelength with a diffraction angles centered around ~75 degrees and with numerical aperture (NA) ~0.5 inside the glass slide. The DOE pattern is shown in the Atomic Force Microscope (AFM) image in Fig. 6(b). The pattern scanned from one edge to another has a chirped period with a value varying from 0.44 nm to 0.5 nm. That introduces a first-order diffraction beam having the desired lensing effect.

The DOE patterns were first developed using a holographic lithography technique,[24,25] where the object beam is created by a positive lens. Hence, DOE's lensing properties (diffraction angle and NA) are controllable through the recording angles, NA of object beam, and recording location with respect to the focus of the object beam. In the holographic setup, a 50 *mW*-HeCd laser with 442-*nm* wavelength was used and the patterns were recorded on a positive photoresist film, Shipley Microposit S1805, coated on a glass substrate. Later, the DOE patterns were integrated on the back-side of the SPR chip using a UV cured nano-imprint technique,[26] where the patterns were replicated from the photoresist mold by casting a PDMS (Polydimethylsiloxane) mold. The PDMS mold is then used to place on the OrmoComp UV curable film coated on the backside of SPR chip. The UV light source (370-*nm* wavelength) was exposed to the film by passing through the transparent PDMS mold and then PDMS mold was peeled off from the substrate.

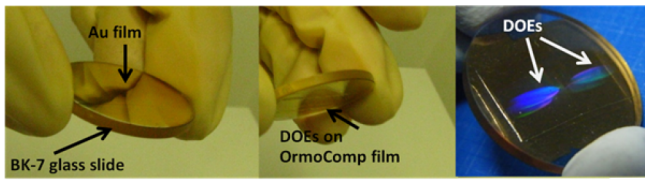

(a)

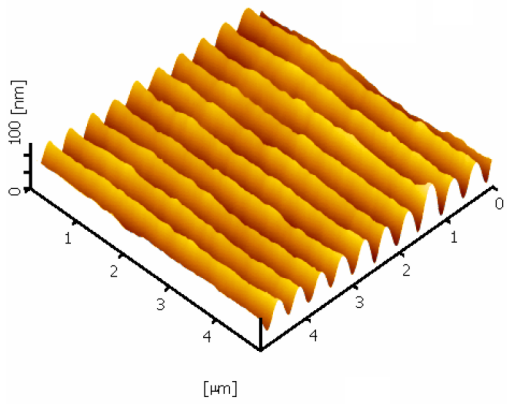

(b)

FIG. 6. Demonstration of integrated DOEs-SPR sensor (a) and atomic forces microscope image of DOE pattern (b).

IV. RESULTS AND DISCUSSIONS

This section demonstrates the experiment on detection of cadmium (Cd^{2+}) ions in water using EF-SPR with a time dynamic detection approach. The cadmium ion solution was prepared by dissolving cadmium chloride ($CdCl_2$) in deionized water with varying concentrations. The measurement is described in section IV A, while the effects of the system parameters on the measurements are included in section IV B and IV C. Finally, low concentration measurements are discussed in section IV C.

A. Time dynamics measurements

In this work, the change in intensity at a desired SPR angle is measured as illustrated in Fig.5(c). Using the proposed system, typical time dynamics is measured as shown in Fig. 7. as a plot of intensity versus time. This measurement is for a high Cd^{2+} ionic concentration (100 ppm). The graph shows the change of the detected reflection upon applying 1Volt potential across the channel. The intensity was found to increase gradually during the ion deposition till it reaches a saturation point. The slope of the curve represents the linear rate of change in the signal with time, which is in agreement to the approximated model expressed in Eqn.(8), where $dShift/dt$ is linearly proportional to the rate of change in volume fraction of the deposited ions (dV_f/dt). The measured response is however not linear. Two main reasons are identified for this nonlinearity: (1) SPR condition shifts out of the detection range of the system and (2) the saturation of ion deposition within the detection region (region of width D on the gold surface) occurs. At saturation point, numerically defined by the time where reflection reaches 90 %, a detectable signal may be out of the detection range of the presented system. This leads to no further dip shift with ionic concentration especially at high concentration ranges. For the cases of saturation, proper detection of high ionic concentration (in the *ppm* range) should be measured by the slope ($dshift/dt$). Higher ionic concentration produces faster SPR response and hence a sharper slope. From experimental observations, saturation was achieved within a second for ionic concentrations in the range of hundreds of *ppm*. Distinguishing different slopes at this high rate with a few sampling points is challenging and can result in large errors. That sets an upper detection value of Cd^{2+}ions to approximately 200 *ppm*.

In the other extreme, measurement of lower ionic concentration (*ppb* range), the slope is very small and it takes longer time to notice the SPR shift. This is due to less amount of ion deposition. The measurement time can be minimized by increasing the applied force on the ions though larger electric field. The force can be increased by applying a higher potential (limited by the hydrolysis of water around 1.1 V) or by reducing the flow channel thickness (d). This leads to a higher sensitivity of the SPR system.

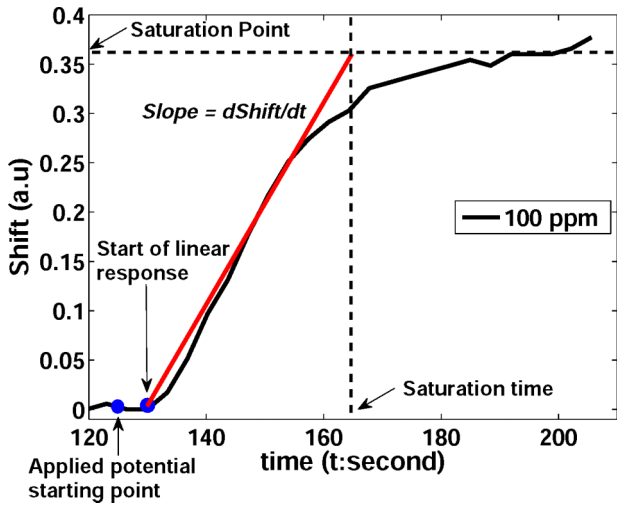

FIG. 7. Time dynamics for the system at ion concentration of 100 ppm and potential application of 1V.

Another point of importance here is the delay between the application of the applied potential and the observation of the response. This delay is due to the time needed to accumulate enough ions on the gold surface that can alter the SPR response. This depends on both the ionic concentration in water (C_0) and the flow rate in the channel (J).

B. Effect of the applied potential

The time dynamics of the SPR intensity for three different potentials of 0.5, 0.8 and 1.1 Volts are used to deposit 10 ppm concentration of Cd^{2+} ions on the sensing surface. Since the applied potential is directly proportional to the SPR response, increasing the potential results in larger number of ions adsorbed on the sensing surface. That increases the sensor response as shown in Fig. 8. The measured change of the slope ($dshift/dt$) varies from 0.0011 s^{-1} at 0.5 V to 0.0036 s^{-1} at 1.1 V. Using Eqn. (8), the corresponding slopes vary from 0.0005 s^{-1} to .0018 s^{-1} at the same potential values. The difference in the calculations and the measurements is due to several approximations used in deriving the model in Eqn.(6). Another source of error is from the application of Maxwell Garnett approximation[22] to detect the effective refractive index. In spite of the errors, the calculated slopes are within the same order of magnitude as the measurements and also, the trend of the change in the calculated slopes matches that of the measurements. An increase in the slope by a factor of 0.0018/0005=3.6 is calculated, while the measured slope increases by 0.0036/.0011=3.273.

C. Low concentration measurements

For low ionic concentration measurements, the applied potential (V) and flow channel thickness (d) are kept at 1.1 Volts and 250 μm, respectively, in order to apply a high electric field to the ions. That allowed time dynamics observations down to ionic concentrations of 250 *ppb* as shown in Fig. 9. The slope of the plot varied from 1.56×10-4 s^{-1} to 1.77×10-5 s^{-1} for ionic concentrations of 1 *ppm* to 250 *ppb*. It is worth mentioning that upon changing the flow rate (J), the linear slope did not seem to change. This agrees well with the approximated model in Eqn. (9) when expanding the concentration C_c according to Eqn. (3) to Eqn. (6).

$$\frac{dV_f}{dt} = J \times C_o \times \frac{d_c}{d} = C_o \times w \times \psi \times E \times D. \tag{10}$$

where $\psi = nq/6\pi r$. As can be observed in Eqn. (10), the slope does not depend on the flow rate (J). However it depends linearly on the applied electric field (E) as well as the initial concentration (C_0).

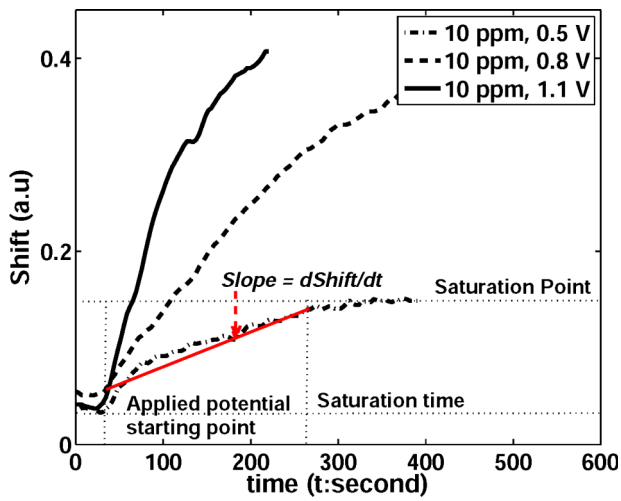

FIG. 8. Time dynamics of ion deposition on the sensing region and the effect of applied voltage.

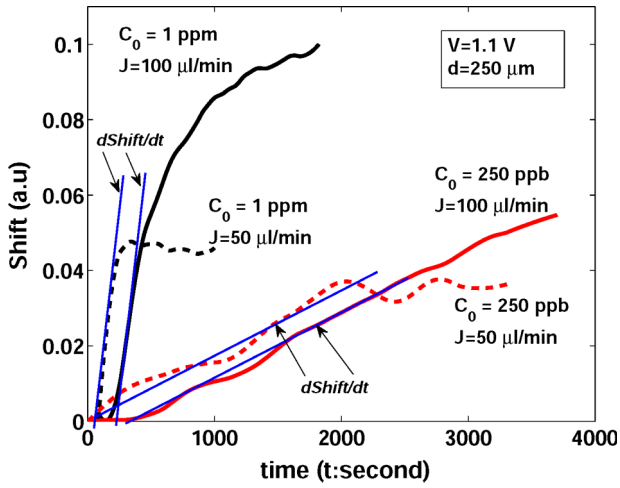

FIG. 9. Effect of reducing channel thickness and flow rate on the measurements and device sensitivity.

At lower flow rate, faster SPR response was observed (smaller delay before starting the linear response) and the signal tends to saturate at an earlier time. Slower flow rate allows a longer interaction time between the ions and the applied electric force at the detection region leading to a faster accumulation of ions which allows earlier start of the linear response compared to fast flow rate. This is shown clearly in Fig. 9 where in the case of 1 *ppm* the response at 50 $\mu l/min$ flow rate starts approximately 40 seconds earlier than that of 100 $\mu l/min$. For the lower concentration of 250 *ppb*, the time shift increases to 100 seconds approximately.

V. CONCLUSIONS

In this work, highly sensitive electric-field assisted SPR system integrated with two Diffractive Optical Elements (DOEs) has been demonstrated for the detection of heavy metal ions in water. With no surface functionalization of the Surface Plasmon Resonance (SPR) substrate, the metal ion can be directed on the sensor surface with the assistance of an external electric field. In addition to tracking SPR shift, the detection scheme focuses on time dynamic measurement. This allows larger detection ranges from *ppb* up to hundreds of *ppm* levels without the concern of saturated ion deposition on an active sensing area or resonance out of the detectable angular spectrum, for example. Optimizing the channel thickness, applied potential and flow rate, both system sensitivity (low concentration detection) and response time (short saturation time) can be realized. Low concentration of cadmium ions in water down to 250 *ppb* was demonstrated. To verify the physics of ion deposition to SPR response, we have presented a first order model for the system where the calculated linear slope shows some agreement with the measurements.

ACKNOWLEDGMENTS

The authors would like to acknowledge financial support from the National Electronic and Computer Technology Center (NECTEC), NSTDA, Ministry of Science & Technology, Royal Thai Government.

[1] R. Singh, N. Gautam, A. Mishra, and R. Gupta, "Heavy metals and living systems: an overview," Indian J Pharmacol. **43**, 246–253 (2011).

[2] A. Tadjarodi, A. Abbaszadeh, M. Taghizadeh, N. Shekari, and A.A. Asgharinezhad, "Solid phase extraction of Cd(II) and Pb(II) ions based on a novel functionalized Fe_3O_4@ SiO_2 core-shell nanoparticles with the aid of multivariate optimization methodology," Materials Science and Engineering C **49**, 416-421 (2015).

[3] Z. Wang, M. Wang, G. Wu, D. Wu, and A. Wu, "Colorimetric detection of copper and efficient removal of heavy metal ions from water by diamine-functionalized SBA-15," Dalton Trans. **43**, 8461-8468 (2014).

[4] H, Qu, L. Cao, G. Su, W. Liu, R. Gao, C Xia, and J. Qin, "Silica-coated ZnS quantum dots as fluorescent probes for the sensitive detection of Pb^{2+} ions," JNanopart Res **16**:2762, 1-12, (2014).
[5] S.A. El-Safty, M. A. Shenashen, M. Ismael, M. Khairy, and M. R. Awual, "Optical mesosensors for monitoring and removal of ultra-trace concentration of Zn(ii) and Cu(ii) ions from water," Analyst **137**, 5278-5290 (2012).
[6] N. Chauhan, S. Gupta, N. Singh, S. Singh, S. S. Islam, K. N. Sood, and R. Pasricha, "Aligned nanogold assisted one step sensing and removal of heavy metal ions," Journal of Colloid and Interface Science **363**, 42-50 (2011).
[7] L. Rottmann and K. G. Heumann, "Determination of heavy metal interactions with dissolved organic materials in natural aquatic systems by coupling a high-performance liquid chromatography system with an inductively coupled plasma mass spectrometer," Anal. Chem. **66**, 3709-3715 (1994).
[8] R. K. Mahajan, I. Kaur, and T. S. Lobana, "A mercury (II) ion-selective electrode based on neutral salicylaldehydethiosemicarbazone," Talanta **59**, 101-105 (2003).
[9] W. J. Yi, Y. Li, G. Ran, H. Q. Luo, and N. B. Li, "Determination of cadmium(II) by square wave anodicstripping voltammetry using bismuth-antimony film electrode," Sensors and Actuators B: Chemical **166-167**, 544-548 (2012).
[10] R.-G. Cao, B. Zhu, J. Li, and D. Xu, "Oligonucleotides-based biosensors with high sensitivity and selectivity formercury using electrochemical impedance spectroscopy," Electrochemistry Communications **11**, 1815-1818 (2009).
[11] L. Sartore, M. Barbaglio, L. Borgese, and E. Bontempi, "Polymer-grafted QCM chemical sensor and application to heavy metal ions real time detection," Sensors and Actuators B: Chemical **155**, 538-544 (2011).
[12] E. Wijaya, C. Lenaerts, S. Maricot, J Hastanin, S. Habraken, J.-P. Vilcot, R. Boukherroub, and S. Szunerits, "Surface plasmon resonance-based biosensors: from the development of different SPR structures to novel surface functionalization strategies," Current Opinion in Solid State and Materials Science **15**, 208-224 (2011).
[13] D. R. Shankaran, K. V. Gobi, and N. Miura, "Recent advancements in surface plasmon resonance immunosensors for detection of small molecules of biomedical, food and environmental interest," Sensors and Actuators B: Chemical **121**, 158-177 (2007).
[14] Y. W. Fen and W. M. M. Yunus, "Surface plasmon resonance spectroscopy as an alternative for sensing heavy metal ions: a review," Sensors Review **33**, 305-314 (2013).
[15] E. S. Forzani, H. Zhang, W. Chen, and N. Tao, "Detection of heavy metal ions in drinking water using a high-resolution differential surface plasmon resonance sensor," Environ. Sci. Technol. **39**, 1257-1262 (2005).
[16] S. Lin, C. C. Chang, and C. W. Lin, "A reversible optical sensor based on chitosan film for the selective detection of copper ions," Biomed.Eng. Appl. Basis Commun. **24**, 453-459 (2012).
[17] L. May May and D. A. Russell, "Novel determination of cadmium ions using an enzyme self-assembled monolayer with surface plasmon resonance," Analytica Chimica Acta **500**, 119-125 (2003).
[18] S. Wang, E. S. Forzani, and N. Tao, "Detection of heavy metal ions in water by high-resolution surface plasmon resonance spectroscopy combined with anodic stripping voltammetry," Anal.Chem. **79**, 4427-4432 (2007).
[19] A. N. Naimushin, S. D. Soelberg, D. U. Bartholomew, J. L. Elkind, and C. E. Furlong, "A portable surface plasmon resonance (SPR) sensor system with temperature regulation," Sensors and Actuators B **96**, 253–260 (2003).
[20] T.M. Chinowsky, S. D. Soelberg, P. Baker, N. R. Swanson, P. Kauffman, A. Mactutis, M. S. Grow, R. Atmar, S. S. Yee, and C. E. Furlong, "Portable 24-analyte surface plasmon resonance instruments for rapid, versatile biodetection," Biosensors and Bioelectronics **22**, 2268–2275 (2007).
[21] S. Boonruang and W.S Mohammed, "Integrated diffractive optical elements for optical sensors applications," in Proceedings of the 2nd International Conference on Photonics (ICP), Kata Kinabalu, Malaysia, 17-19 October 2011, pp.1-5.
[22] G. J. C. Maxwell, "Colours in metal glasses and metal films," Philos. Trans. R. Soc. London, Sect. A **3**, 385–420 (1904).
[23] U. Kreibig and M. Vollmer, *Optical properties of metal clusters* (Springer, 1995), Vol. 25.
[24] P. Junlabhut, S. Phoojaruenchanachai, W. Pecharapa, and S. Boonruang, "Fabrication of holographic lens as a coupling device in surfaceplasmon resonance biosensor," Proc. of SPIE **7743**, 774302 (2010).
[25] H.C. Pederson and C. Thirstrup, "Design of near-field holographic optical elements by Grating Matching," Appl. Opt. **43**, 1209–1215 (2004).
[26] M. Bender, A. Fuchs, U. Plachetka, and H. Kurz, "Status and prospects of UV-Nanoimprint technology," Microelectronics Engineering **83**, 827-830 (2006).